Pellet Fuelling and ELMy H-mode Physics in JET

The JET Team[1], prepared by L.D. Horton 1)

JET Joint Undertaking, Abingdon, U.K.
1) present address: Max-Planck-Institut für Plasmaphysik, Garching, Germany

e-mail contact of main author: Lorne.Horton@ipp.mpg.de

Abstract. As the reference operating regime for ITER, investigations of the ELMy H-mode have received high priority in the JET experimental programme. Recent experiments have concentrated in particular on operation simultaneously at high density and high confinement using high field side (HFS) pellet launch. The enhanced fuelling efficiency of HFS pellet fuelling is found to scale favourably to a large machine such as JET. The achievable density of ELMy H-mode plasmas in JET has been significantly increased using HFS fuelling although at the expense of confinement degradation back to L-mode levels. Initial experiments using control of the pellet injection frequency have shown that density and confinement can simultaneously be increased close to the values necessary for ITER. The boundaries of the available ELMy H-mode operational space have also been extensively explored. The power necessary to maintain the high confinement normally associated with ELMy H-mode operation is found to be substantially higher than the H-mode threshold power. The compatibility of ELMy H-modes with divertor operation acceptable for a fusion device has been studied. Narrow energy scrape-off widths are measured which place stringent limits on divertor power handling. Deuterium and tritium codeposition profiles are measured to be strongly in/out asymmetric. Successful modelling of these profiles requires the inclusion of the (measured) scrape-off layer flows and of the production in the divertor of hydrocarbon molecules with sticking coefficients below unity. Helium exhaust and compression are found to be within the limits sufficient for a reactor.

1. Introduction

The ELMy H-mode regime is the reference operating regime for ITER. Nevertheless, an integrated demonstration of the parameters necessary for the successful operation of ITER does not exist. Indeed, such a demonstration has been shown to be in principle impossible due to the different scalings one would expect for different regions of the plasma [1]. Furthermore, confidence in the extrapolation to a next step device is low for some parameters such as the density limit and the ELM size. For this reason high priority in the programme of the JET Joint Undertaking in its last years was given to the study of the ELMy H-mode, its scaling and the compatibility of its various positive characteristics with one another.

In Section 2 the results are presented of experiments to study HFS pellet injection using the new in-vessel guide tube. HFS pellet fuelling efficiency is compared to that of pellets injected from the low field side (LFS). The question of H-mode access and, in particular, the power necessary to obtain ELMy H-modes with good confinement is discussed in Section 3. Experiments to study the compatibility of ELMy H-mode operation with acceptable divertor operation are presented in Section 4 and a summary and status are given in Section 5.

The results presented here can only be a brief summary of the experiments carried out on ELMy H-mode physics by Task Force P of the JET Joint Undertaking. With the winding up of the Joint Undertaking it was recognised that there was an obligation to provide the experimental results in a form usable by the fusion community and funds were set aside to pay for analysis of the data. The results of this analysis are the basis for this paper. The full report can be found in [2].

[1] A list of the JET Team members can be found in the overview paper OV1/2.

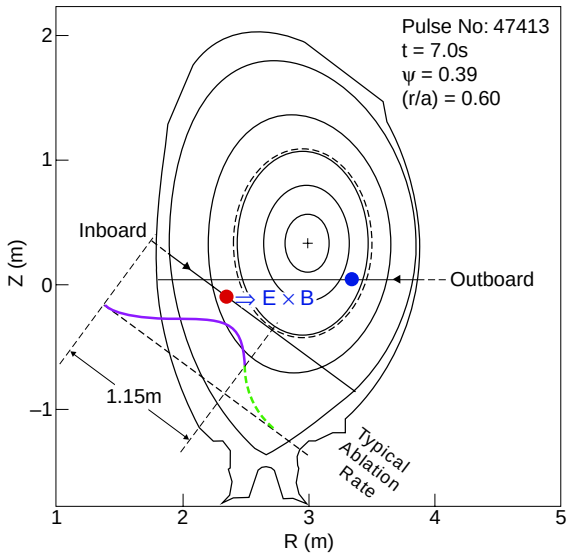

FIG. 1. Injection geometries of the JET centrifuge pellet injector.

2. High Field Side Pellet Fuelling

During a short shutdown in the summer of 1999, a pellet guide tube was installed in the JET torus, allowing injection of pellets into the plasma from the high field side (HFS) of the machine [3]. A series of experiments were then carried out in the autumn of 1999 to test the efficiency of HFS pellet fuelling and to compare it with conventional LFS fuelling. The two injection geometries are shown in Fig. 1.

The HFS injection path does not pass through the plasma centre in order to maximise the radius of curvature of the in-vessel guide tube. Tests carried out by ORNL on a full scale mock-up of the guide tube had shown that the maximum injection velocity, v_{inj}, for 100% probability of survival was 160 m/s [4]. This result was confirmed by scans of pellet injection speed into L-mode plasmas. Therefore the majority of the experiments comparing HFS and LFS fuelling comparisons were performed with v_{inj}=160 m/s.

2.1 Physics of Pellet Deposition

Injection of pellets from the magnetic high field side has been shown first on ASDEX Upgrade [5] and then on DIII-D [6] to greatly improve fuelling efficiency over injection from the low field side. This improvement is due to a magnetic force which pushes the high beta plasmoid created by the ablating pellet towards lower magnetic field and thus to higher major radius. The resulting displacement causes prompt particle losses for low field side injection and results in more central fuelling when the pellet is ablated on the low major radius side of the plasma magnetic axis. In order to test the scaling of this physics to larger machines (and thus, to some extent, its applicabillity to next step devices), similar experiments have been carried out on JET [7].

In Fig. 2 the increment in electron density caused by a HFS pellet is shown for two L-mode discharges at different input powers. Also shown is the D_α emission from the ablation of each pellet mapped from time onto minor radius using the pellet injection velocity and geometry. In the lower power pulse, Fig. 2(a), the pellet reaches and passes the tangency point of its trajectory before being completely ablated and the D_α emission folds back to higher minor radius. Despite the pellet tangency point being at $\rho \sim 0.7$ for these pulses, the electron density further towards the plasma core is seen to rise significantly in a time interval shorter than normal diffusive transport times. This rise in the density in the region ρ=0.3-0.7 is consistent with a rapid displacement of the pellet mass towards lower magnetic field as seen in AUG Upgrade and DIII-D.

The core fuelling shown in Fig. 2 for HFS pellets is not observed with LFS pellets except at very low input power (P<3 MW) where the usual ablation models predict deep penetration. Indeed, for HFS pellets, the fraction of the particle fuelling inside ρ=0.7 is found to remain

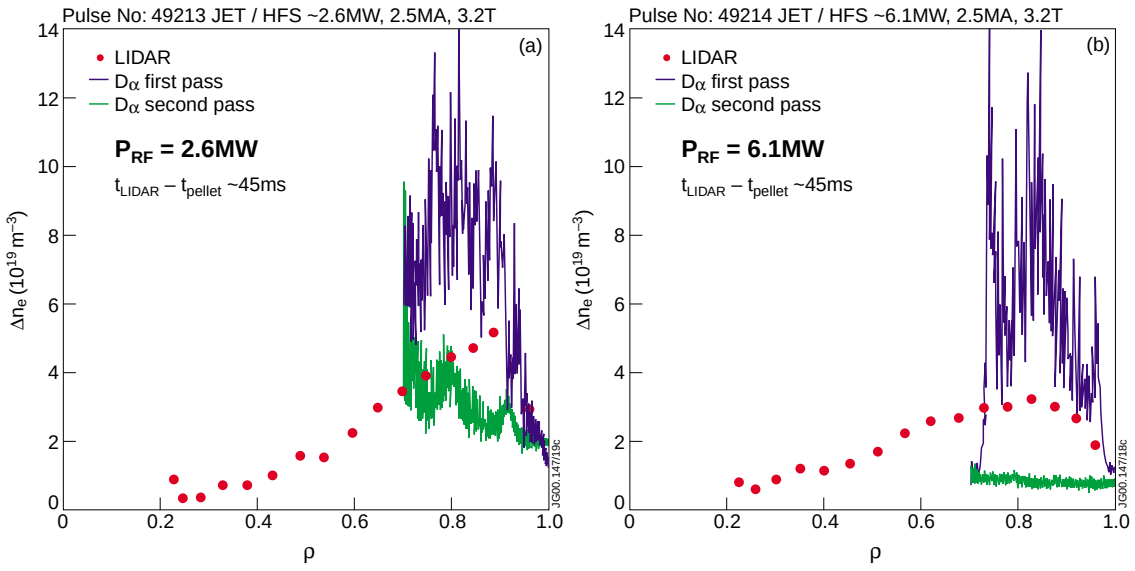

FIG. 2. Increase in electron density caused by HFS pellets injected into L-mode plasmas with (a) 2.6 MW of input power and (b) 6.1 MW. Also shown are the measured D_α ablation profiles mapped from time onto normalised minor radius.

about constant as the input power is increased (Fig. 2(b)) [7]. Thus it appears that for HFS pellets the increased pellet ablation rate observed at higher temperature is compensated by an increased displacement of the pellet produced plasmoid. This is consistent with models of pellet acceleration which predict increased pellet displacement at higher pressure (and thus input power) [8]. Additional experiments to test the influence of magnetic field and of safety factor on the pellet particle deposition profile showed no strong dependence.

2.2 H-mode Density Limit Studies

The density achievable in JET ELMy H-modes using gas fuelling is limited by a degradation of confinement and a back transition to L-mode conditions. At normal current and field (2.5 MA, 2.5 T) the achievable density is somewhat below the Greenwald density, $n_G[10^{20} m^{-3}]=I[MA]/\pi a[m]^2$ [9]. Some improvement is obtained by shaping the plasma. Since the confinement degradation is linked to a reduction of the edge pressure at high edge density while improved fusion performance is tied to high core density, core fuelling with HFS pellets, thus peaking the density profile, is an attractive scenario for a fusion reactor.

Initial experiments with HFS pellet injection into ELMy H-modes have indeed produced plasmas with very high densities (Fig. 3) [10]. Densities as high as $1.6 \cdot n_G$ have been obtained. The confinement degradation observed with HFS pellets appears to be similar to that seen previously with gas fuelling, although the range of accessible densities has been extended. It is to be noted, however, that the degradation in confinement enhancement factor seen in Fig. 3 is in part due to the positive density dependence predicted by present one term confinement scalings. The degradation of the energy confinement, as opposed to the confinement enhancement factor, is rather less than that shown in Fig. 3. Nevertheless, above $n/n_G \sim 0.8$ there is a strong reduction in the absolute confinement as well, leading to parameters which are probably uninteresting for a fusion device. This was observed despite the fact that strongly peaked density profiles have been obtained, especially at high density (density peaking, $n_{e0}/\langle n_e \rangle \leq 1.8$ at $n/n_G \sim 1.6$).

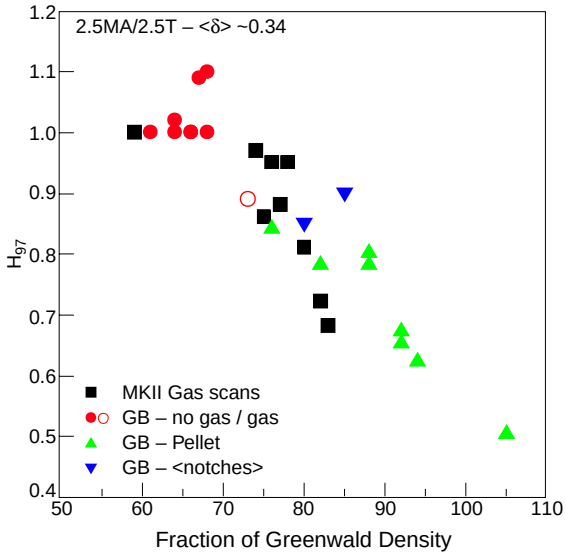

FIG.3. Confinement enhancement factor versus normalised line averaged density for a variety of JET ELMy H-mode discharges.

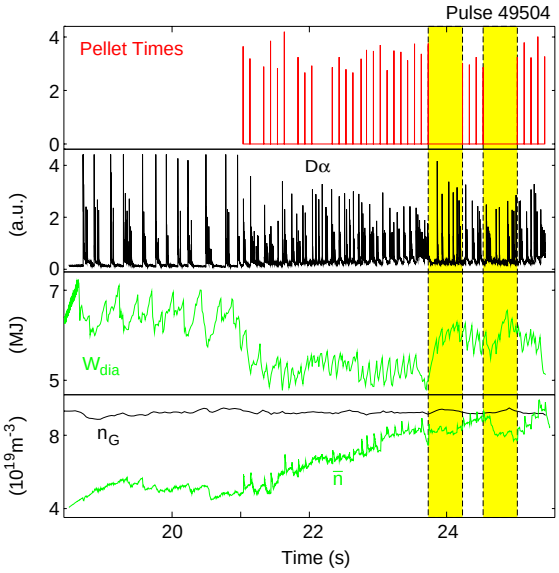

FIG. 4. Time traces of a 2.5 MA, 2,4 T ELMy H-mode discharge, heated by 15 MW of neutral beam power and fuelled with 10 Hz HFS pellets. The shaded intervals correspond to interuptions or notches in the pellet string.

The combined density and confinement behaviour can be improved by controlling the pellet injection frequency at high density. Initial experiments using interruptions in the pellet strings have resulted in improved performance [11]. An example of the time histories of such a pulse is shown in Fig. 4. In this pulse the density was initially raised using a continuous 10 Hz string of HFS pellets. At high density and relatively poor confinement the pellet string was repetitively interrupted (the shaded areas in Fig. 4). The stored energy recovered to nearly the value obtained at low density with no fuelling while the density remained high. Two further bursts of pellet fuelling after the interruptions are sufficient to maintain the high density while not seriously degrading the confinement. In this way it has been possible to maintain discharges at 85-90% of the Greenwald density with little degradation in confinement as compared to unfuelled discharges (the blue inverted triangles in Fig. 3).

3. H-mode Access

The power necessary to obtain and maintain an ELMy H-mode forms one of the boundaries of the operation space of ITER. Exactly how this power scales to large machines is thus a key input to the ITER design. A large range of experiments on JET have shown that the H-mode threshold scaling laws are insufficient to describe this boundary, even in present day machines. In particular the H-mode threshold in JET is found to depend strongly on divertor geometry, a parameter which is difficult to include in empirical scalings [12].

Of further concern is the observation that the power necessary to obtain and maintain the best ELMy H-mode confinement in JET is substantially above the conventional H-mode threshold power [13]. In JET, the best ELMy H-mode confinement is obtained in discharges with regular Type I ELMs and the power necessary to maintain such ELMs is labelled the Type I ELM threshold power. This power scales in a similar manner to the H-mode threshold power, increasing with magnetic field and density (or with current which is colinear with density in

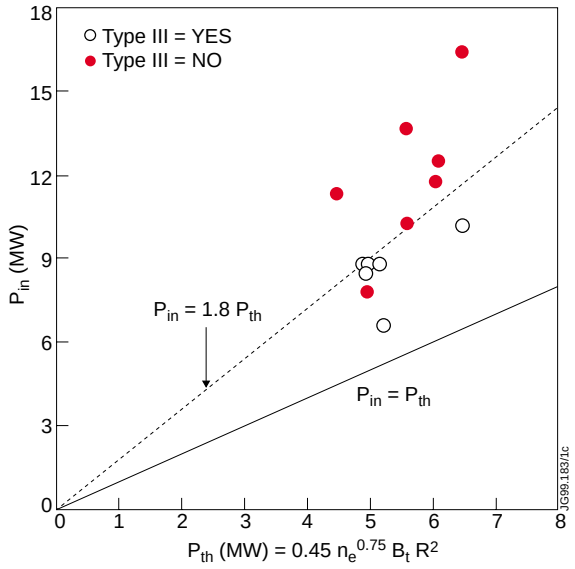

FIG. 5. Input power versus H-mode threshold power for a series of steady ELMy H-mode discharges. The pulses which contain phases of Type III ELMs are shown as open circles, those with uniquely Type I ELMs as closed circles.

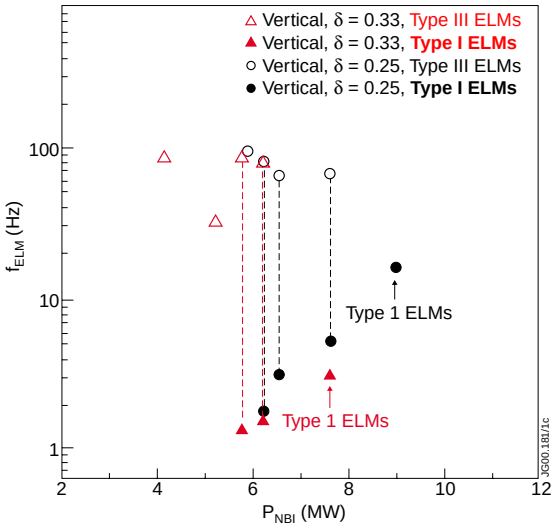

FIG. 6. ELM frequency versus neutral beam input power for a series of ELMy H-mode discharges. Discharges which alternate between Type I and Type III ELMs are shown with two points linked with a vertical dashed line.

our data), but is almost a factor of two higher (Fig. 5) [14]. It appears that increased plasma triangularity reduces somewhat the Type I ELM threshold (Fig. 6) which however remains at least 50% above the H-mode threshold power.

4. Divertor Issues

The compatibility of ELMy H-mode operation with acceptable divertor operation remains one of the most important outstanding problems in defining an integrated scenario for a next step machine. In particular, while the core plasma confinement and density are maintained, the divertor must successfully exhaust the power and particles escaping from the plasma. Furthermore, the erosion and redeposition of divertor and first wall material must be compatible with an acceptable availability of a fusion power plant while the inventory of tritium in the machine remains at safe levels.

4.1 Divertor Energy Deposition Profile

One of the most demanding limitations on ELMy H-mode operation is the power deposition on the divertor, particularly during ELMs. In order to provide a reasonable divertor lifetime, the energy density deposited on the divertor by an ELM must be below the ablation threshold for the divertor material. The profile of the energy deposition on the divertor is thus important in predicting divertor lifetimes. In JET, a series of experiments to measure the divertor energy deposition profile have been performed using shot-to-shot shifts in the divertor strike point position and thermocouples embedded in the divertor tiles [15]. Since the tiles in the JET Mark II divertors are cooled only by radiation between pulses, the thermocouples provide a good measure of the energy deposited on the tile integrated throughout the pulse. By positioning the divertor strike point near the joint between two tiles, it is possible to deduce the average power scrape off width in a given pulse. With a series of slightly shifted pulses, a power profile can be constructed.

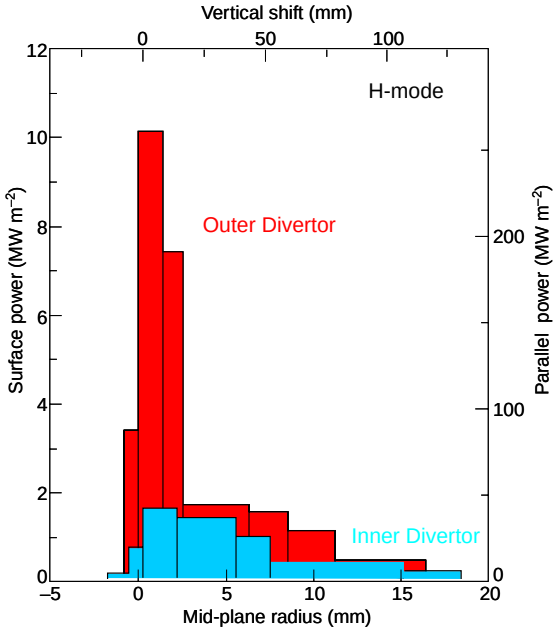

FIG. 7. Divertor power deposition profiles, averaged over the 12 MW heating pulse, measured using divertor thermocouples and pulse-to-pulse shifts in the divertor strike point positions.

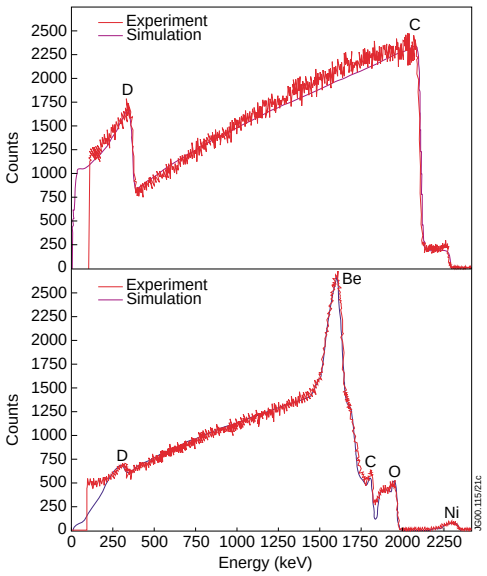

FIG. 8. Rutherford backscattering spectra from (a) a Mark IIGB tile in a shadowed region of the inner divertor and (b) from an exposed region.

The power density profiles from a series of unfuelled ELMy H-modes are shown in Fig. 7 for the inner and outer divertor targets. The most striking feature of the profiles is the strong asymmetry between inner and outer target with roughly two thirds of the power flowing to the outer target. This asymmetry is greater than what one would expect from the ratio of surface areas on the outer and inner sides of the main plasma, for example. The extra power on the outer target is concentrated in a thin layer, about 2-3 mm when mapped to the SOL outer midplane, and even in JET results in power densities which would be difficult to sustain with an actively cooled divertor. The JET SOL is nearly collisionless near the separatrix and losses of ions from the core plasma which then directly impinge on the divertor are being considered as an explanation for this sharp power feature. Such ion losses fall predominantly on the outer divertor target with the normal direction of plasma current in JET. Preliminary experiments with reversed current and field show a much more symmetric power deposition on the divertor and further, more detailed experiments are planned in the near future.

4.2 Tritium Codeposition

Following the JET DTE1 experiment, large amounts of tritium were found to remain in the vacuum vessel [16]. Currently 2 g remain of the 35 g of tritium which entered the vacuum vessel [17]. This tritium is thought to be tied up in thick codeposited layers, which initially formed on shadowed regions of the inner divertor and then spalled from the surfaces and fell to the bottom of the vacuum vessel. Analysis of deposits on the inner wall of the JET Mark IIGB divertor have shown that the deposits are rich in beryllium and intermediate Z metals in areas which are exposed to the plasma and are composed almost entirely of carbon and deuterium in shadowed regions of the divertor (Fig. 8) [17]. This implies that the carbon which was originally deposited on the exposed areas of the divertor has subsequently been resputtered and then migrates as a (partially) recycling hydrocarbon to non-exposed surfaces.

Successful modelling of the strong in/out asymmetry of the deuterium codeposition and of the large deposits in shadowed areas of the inner divertor requires three ingredients not normally included in edge codes: (a) a strong SOL flow from the outer to inner divertor; (b) enhanced sputtering of carbon from the inner wall compared to the normal 2D models; and (c) recycling impurities, probably in the form of hydrocarbons, especially in the inner divertor region.

The strong SOL flow has been measured in JET [18] and can be qualitatively reproduced by fluid codes which contain the drift terms. Unfortunately, computational difficulties remain in combining these drifts with impurity simulations and further work is required before a self-consistent picture for the in/out impurity asymmetry is produced. Enhanced wall sputtering is consistent with the large quantity of deposited carbon found in the divertor, larger than can have been sputtering from the divertor itself. Indeed, the apparently predominant role of the first wall in providing the carbon for codeposition makes the replacement of the first wall with a metal such as beryllium while maintaing the carbon divertor an interesting potential experiment. Finally, the hydpothesis of recycling hydrocarbons is supported by recent laboratory measurements [19] which show that heavy hydrocarbon radicals can indeed have a low sticking probability. Thus the elements necessary for modelling the deposition appear to be in place. Integration of these elements into a self-consistent plasma/wall model is ongoing.

4.3 Helium Exhaust and Compression

A series of helium exhaust and compression experiments have been performed to study the compatibility of JET ELMy H-modes with the exhaust of helium ash necessary for a reactor. Helium exhaust efficiency is ususally characterised in terms of the Reiter-Wolf-Kever criterion [20], τ_{He}^*/τ_E, where τ_{He}^* is the helium exhaust time and τ_E is the energy confinement time. $\tau_{He}^*/\tau_E<15$ is required to allow ignition in a reactor and lower values allow a wider operating space. Previous results from DIII-D [21], AUG [22] and JT-60U [23] have shown that the helium exhaust from ELMy H-modes is sufficient in this sense. Using argon frosting of the divertor cryopump to exhaust helium, similar experiments have now been performed on JET with $\tau_{He}^*/\tau_E\sim7.6$ in the best cases [24].

One difficulty with this figure-of-merit is its extrapolability to very large machines such as ITER. Simulations [25] show that, at high density, the scale length of the divertor becomes larger than the neutral helium mean free path only in ITER scale devices. In smaller machines, including JET, the approach to high density and detachment leads to an increasing neutral helium penetration into the core plasma and thus lower divertor enrichment [26]. In ITER, where the pumping is from the private flux region, increased detachment allows more helium to reach the pumps while not significantly increasing leakage from the divertor. Thus the helium enrichment is predicted to increase with density.

5. Summary

In as much as is possible given the fundamental difficulties in scaling present results, the applicability of the ELMy H-mode as an integrated operating scenario for ITER has been studied in a wide range of experiments at JET. The initial results using HFS pellet injection are encouraging and further experiments are planned to demonstrate long pulse operation at the required densities and temperatures. Access to the high confinement H-mode regime has been identified as a key issue with the conventional H-mode threshold scalings perhaps providing a too optimistic prediction. Finally, compatibility with successful divertor operation

has been examined. Measurements of narrow power deposition profiles provide a stringent constraint on divertor power handling, at least in low to medium density regimes. Tritium codeposition has also been measured and can be understood by adding new ingredients to the standard divertor/SOL models. The figure-of-merit for helium exhaust is measured to be sufficient for a reactor, as has been the case in other machines with ELMy H-mode regimes.

References

[1] Comments on Plasma Phys. and Controlled Fusion **15** (1994) 359.
[2] MANY AUTHORS, "Descriptive Analysis of 1999 Task Force P data", JET Report JET-R(00)02.
[3] WATSON, M.J., et al., "Improvement, Commissioning and Operation of the JET Pellet Centrifuge", JET Report JET-CP(99)34.
[4] BAYLOR, L.R. and COMBS, S.K., personal communication, 1999.
[5] LANG, P.T., et al., Phys. Rev. Lett. **79** (1997) 1487.
[6] BAYLOR, L.R., et al., in Controlled Fusion and Plasma Physics (Proc. 26th Eur. Conf. Maastricht, 1999), Vol. 23J, European Physical Society, Geneva (1999) 297.
[7] JONES, T.T.C., et al., to appear in Controlled Fusion and and Plasma Physics (Proc. 27th Eur. Conf. Budapest, 2000), paper OR.004.
[8] PARKS, P.B., SESSIONS, W.D. and BAYLOR, L.R., in Controlled Fusion and Plasma Physics (Proc. 26th Eur. Conf. Maastricht, 1999), Vol. 23J, European Physical Society, Geneva (1999) 1217.
[9] SAIBENE, G., et al., Nucl. Fusion **39** (1999) 1133.
[10] SAIBENE, G. and JONES, T.T.C., Chapter 2 in [1].
[11] LANG, P.T., et al., to appear in Controlled Fusion and and Plasma Physics (Proc. 27th Eur. Conf. Budapest, 2000), paper P3.045.
[12] RIGHI, E., et al., poster EXP5/31, this conference.
[13] SARTORI, R., et al., in Controlled Fusion and Plasma Physics (Proc. 26th Eur. Conf. Maastricht, 1999), Vol. 23J, European Physical Society, Geneva (1999) 197.
[14] SARTORI, R., Chapter 6 in [1].
[15] MATTHEWS, G.F., et al., to appear in J. Nucl. Mater. (Proc. 14th Int. Conf. on Plasma Surface Interactions), paper O-4.2.
[16] ANDREW, P.L., et al., Fusion Energy Design **47** (1999) 233.
[17] COAD, J.P., et al., to appear in J. Nucl. Mater. (Proc. 14th Int. Conf. on Plasma Surface Interactions), paper I-2.1.
[18] CHANKIN, A.V., et al., to appear in J. Nucl. Mater. (Proc. 14th Int. Conf. on Plasma Surface Interactions), paper I-4.1.
[19] VON KEUDELL, A., HOPF, C., SCHWARZ-SELINGER, T., JACOB, W., Nucl. Fusion **39** (1999) 1451.
[20] REITER,D., WOLF, G.H., KEVER, H., Nucl. Fusion **30** (1990) 2141.
[21] WADE, M.R., et al., Phys. Plasmas **2** (1995) 2357.
[22] BOSCH, H.S., et al., J. Nucl. Mater **241-243** (1997) 82.
[23] SAKASAI, A., et al., to appear in J. Nucl. Mater. (Proc. 14th Int. Conf. on Plasma Surface Interactions), paper O-9.1.
[24] STORK, D., et al., in Controlled Fusion and Plasma Physics (Proc. 26th Eur. Conf. Maastricht, 1999), Vol. 23J, European Physical Society, Geneva (1999) 205.
[25] KUKUSKIN, A., personal communication based on ITER Divertor Expert Group presentation, Dec. 1999 (Naka).
[26] GROTH, M., et al., to appear in J. Nucl. Mater. (Proc. 14th Int. Conf. on Plasma Surface Interactions), paper P-3.48.